Supplementary Materials

Nanocatalytic Enhancement of Local Heat Transfer in Continuous-Flow Thermal Reactors

Nasser Zouli [1,2], Nujud Maslamani [3], Ayman Yousef [1,5,*] and Muthanna Al-Dahhan [3,*]

[1] Department of Chemical Engineering, College of Engineering and Computer Science, Jazan University, Jazan 11451, Saudi Arabia; nizouli@jazanu.edu.sa
[2] Nanotechnology Research Unit, Jazan University, P.O. Box 114, Jazan 45142, Saudi Arabia
[3] Department of Physical Sciences, Chemistry Division, College of Science, Jazan University, P.O. Box 114, Jazan 45142, Saudi Arabia; naslaman@jazanu.edu.sa
[4] Engineering and Technology Research Center, Jazan University, P.O. Box 114, Jazan 82817, Saudi Arabia
[5] Linda and Bipin Doshi Department of Chemical & Biochemical Engineering, Missouri S&T,
Rolla, MO 65409, USA
* Correspondence: aymanhassan@jazanu.edu.sa (A.Y.); adahhan@mst.edu (M.A.-D.)

List of Abbreviations and Symbols

Note: *For complete nomenclature and definitions, please refer to the main manuscript.*

Abbreviations

Abbreviation	Definition
DW	Deionized Water
HTC	Heat Transfer Coefficient
LF	Laminar Flow regime
LHTC	Local Heat Transfer Coefficient
NF	Nanofluid
NPs	Nanoparticles
Re	Reynolds Number
TC	Thermal Conductivity
TF	Turbulent Flow regime

Symbols

Symbol	Definition	Unit
δ	Thermal length scale, defined as k/h	mm
Φ	Volume fraction of nanoparticles	vol.%
h	Heat transfer coefficient	W/m².K
k	Thermal conductivity	W/m.K

Table S1: Empirical LHTC correlations

Dittus-Boelter correlation	$Nu = 0.023\ Re^{0.87}\ Pr^{0.3}$	(S1)

Gnielinski correlation [26]	$Nu = 0.012\ (Re^{0.87} - 280)Pr^{0.3}$	(S2)
Xuan-Qiang correlation [42] (For laminar conditions)	$Nu = 0.4328(1 + 11.285\ \varphi^{0.754}Pe^{0.218})Re^{0.333}Pr^{0.4}$	(S3)
Xuan-Qiang correlation [42] (For Turbulent conditions)	$Nu = 0.0059(1 + 7.6286\ \varphi^{0.6886}Pe^{0.001})Re^{0.9238}Pr^{0.4}$	(S4)

Table S2: Improvement of the LHTC for Al_2O_3/DW NF of 30 nm for LF regime at Re=1000 and 25°C

Φ of Al_2O_3 NPs (vol.%)	TC of Al_2O_3/DW NFs (W/m.K)	Heat transfer coefficient ($W/m^2.K$)	δ (mm)	Enhancement (k) (%)	Enhancement (h) (%)	Decrease (δ) (%)
0	0.595	526	1.13	0	0	0
0.01	0.608	552	1.10	2	5	2
0.02	0.624	565	1.10	5	7	2
0.03	0.638	584	1.09	7	11	3
0.04	0.652	601	1.08	9.5	14	4
0.05	0.667	620	1.07	12	18	5

Table S3: Improvement of the LHTC for Al_2O_3/DW NF of 30 nm for TF regime at R_e=2800 and 25°C

Concentration of Al_2O_3 NPs (vol.%)	TC of Al_2O_3/DW NFs (W/m.K)	HTC ($W/m^2.K$)	δ (mm)	Enhancement (k) (%)	Enhancement (h) (%)	Decrease (δ) (%)
0	0.595	1410	0.42	0	0	0
0.01	0.608	1530	0.39	2	8.5	7
0.02	0.624	1625	0.38	5	15	9
0.03	0.638	1705	0.37	7	21	11
0.04	0.652	1745	0.37	9.5	24	11
0.05	0.667	1820	0.36	12	29	13

Table S4: Improvement of the LHTC for Al_2O_3/DW NF of 30 nm for TF regime at Re=10000 and 55°C.

Φ of Al_2O_3 NPs (vol.%)	TC of Al_2O_3/DW NFs (W/m.K)	HTC ($W/m^2.K$)	δ (mm)	Enhancement (k) (%)	Enhancement (h) (%)	Decrease (δ) (%)
0	0.639	2270	0.28	0	0	0
0.01	0.657	2645	0.25	3	16	12
0.02	0.683	2837	0.24	7	24	15
0.03	0.707	3020	0.23	11	33	16
0.04	0.734	3148	0.23	15	38	16
0.05	0.759	3275	0.23	19	44	16

Table S5: Improvement of the LHTC for CuO/DW NF of 30 nm for LF regime at Re=1000 and 25°C.

Φ of CuO NPs (vol.%)	TC of CuO/DW NFs (W/m.K)	HTC ($W/m^2.K$)	δ (mm)	Enhancement (k) (%)	Enhancement (h) (%)	Decrease (δ) (%)
0	0.595	526	1.13	0	0	0
0.01	0.629	580	1.08	5	10	4
0.02	0.644	612	1.05	8	16	7
0.03	0.659	650	1.01	10	23	10
0.04	0.668	682	0.98	12	29	13
0.05	0.686	700	0.98	15	33	13

Table S6: Improvement of the LHTC for CuO/DW NF of 30 nm for TF regime at Re=2800 and 25°C.

Φ of CuO NPs (vol.%)	TC of CuO/DW NFs (W/m.K)	HTC ($W/m^2.K$)	δ (mm)	Enhancement (k) (%)	Enhancement (h) (%)	Decrease (δ) (%)
0	0.595	1410	0.42	0	0	0
0.01	0.629	1587	0.39	5	12	7
0.02	0.644	1710	0.38	8	21	9
0.03	0.659	1815	0.36	10	28	13
0.04	0.668	1874	0.35	12	32	16
0.05	0.686	1935	0.35	15	37	16

Table S7: Improvement of the LHTC for CuO/DW NF of 30 nm for TF regime at Re=10000 and 55°C.

Φ of CuO NPs (vol.%)	TC of CuO/DW NFs (W/m.K)	HTC ($W/m^2.K$)	δ (mm)	Enhancement (k) (%)	Enhancement (h) (%)	Decrease (δ) (%)
0	0.639	2270	0.28	0	0	0
0.01	0.690	2815	0.25	8	24	12
0.02	0.732	3015	0.24	14	32	15
0.03	0.768	3185	0.24	20	40	15
0.04	0.782	3276	0.23	22	45	16
0.05	0.798	3480	0.22	25	53	19

Table S8: Improvement of the LHTC for Fe_2O_3/DW NF of 30 nm for LF regime at Re=1000 and 25°C.

Φ of Fe_2O_3 NPs (vol.%)	TC of Fe_2O_3/DW NFs (W/m.K)	HTC ($W/m^2.K$)	δ (mm)	Enhancement (k) (%)	Enhancement (h) (%)	Decrease (δ) (%)
0	0.595	526	1.13	0	0	0
0.01	0.618	561	1.10	3	6	2
0.02	0.6301	585	1.07	6	11	5
0.03	0.647	625	1.03	8	18	8
0.04	0.656	652	1.00	10	23	11
0.05	0.675	680	1.00	13	29	11

Table S9: Improvement of the LHTC for Fe_2O_3/DW NF of 30 nm for TF regime at Re=2800 and 25°C.

Φ of Fe_2O_3 NPs (vol.%)	TC of Fe_2O_3/DW NFs (W/m.K)	HTC ($W/m^2.K$)	δ (mm)	Enhancement (k) (%)	Enhancement (h) (%)	Decrease (δ) (%)
0	0.595	1410	0.42	0	0	0
0.01	0.618	1561	0.39	3	10	7
0.02	0.6301	1673	0.37	6	16	11
0.03	0.647	1786	0.36	8	27	13
0.04	0.656	1838	0.35	10	37	16
0.05	0.675	1897	0.35	13	52	16

Table S10: Improvement of the LHTC for Fe_2O_3/DW NF of 30 nm for TF regime at Re=10000 and 55°C.

Φ of Fe_2O_3 NPs (vol.%)	TC of Fe_2O_3/DW NFs (W/m.K)	HTC ($W/m^2.K$)	δ (mm)	Enhancement (k) (%)	Enhancement (h) (%)	Decrease (δ) (%)
0	0.639	2270	0.28	0	0	0
0.01	0.685	2785	0.25	7	22	12
0.02	0.701	2918	0.24	10	28	15
0.03	0.732	3143	0.23	14	38	16
0.04	0.762	3284	0.23	19	43	16
0.05	0.776	3401	0.23	21	50	16

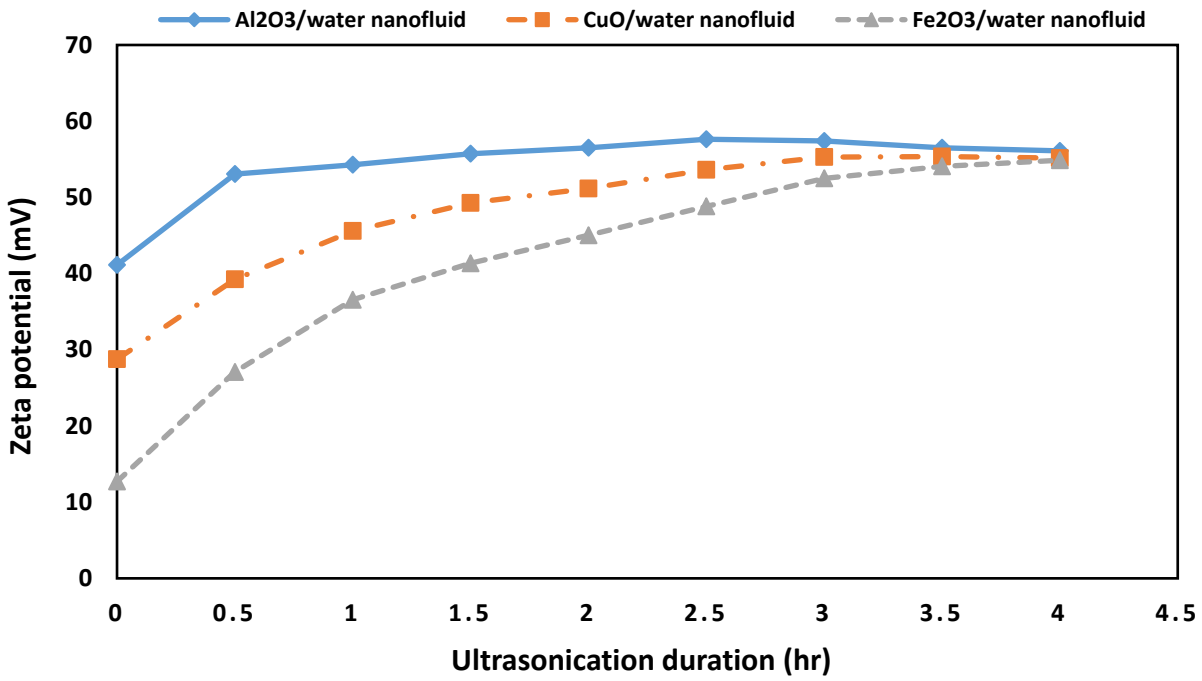
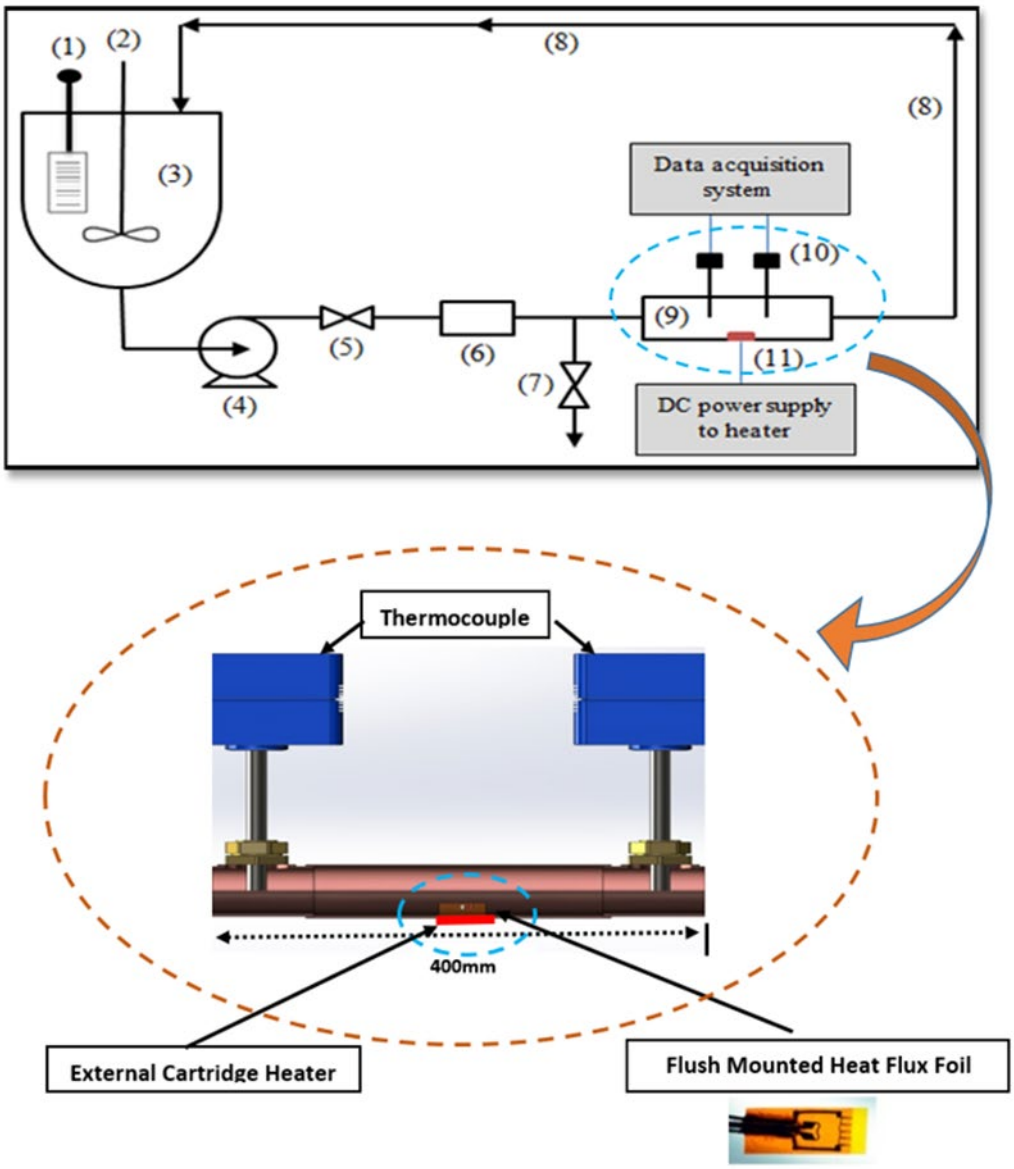


Figure S1: Zeta potentials of NFs after varying ultrasonication durations.



(1) Heater, (2) Agitator, (3) Reservoir tank, (4) Pump, (5) Needle valve, (6) Flow meter, (7) Drainage valve, (8) Copper tube, (9) Test section of copper tube, (10) Thermocouples, (11) Heat flux foil sensor.

Figure S2: Schematic diagram of experimental setup

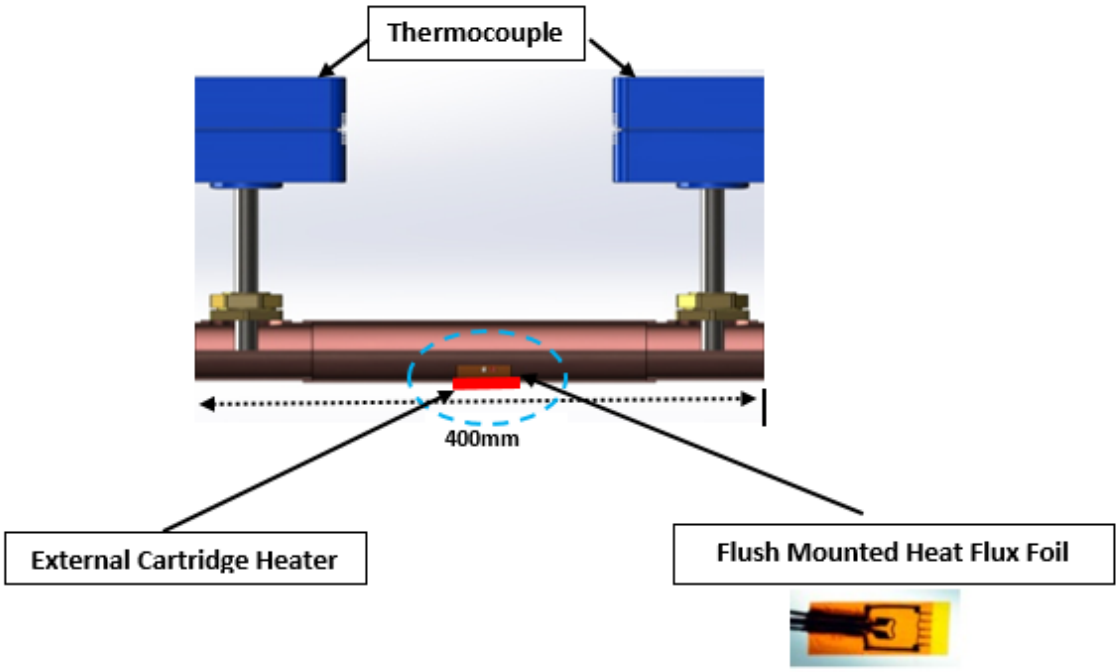


Figure S3: Schematic diagram of the non-invasive heat transfer coefficient probe (flush-mounted on the inner wall surface)

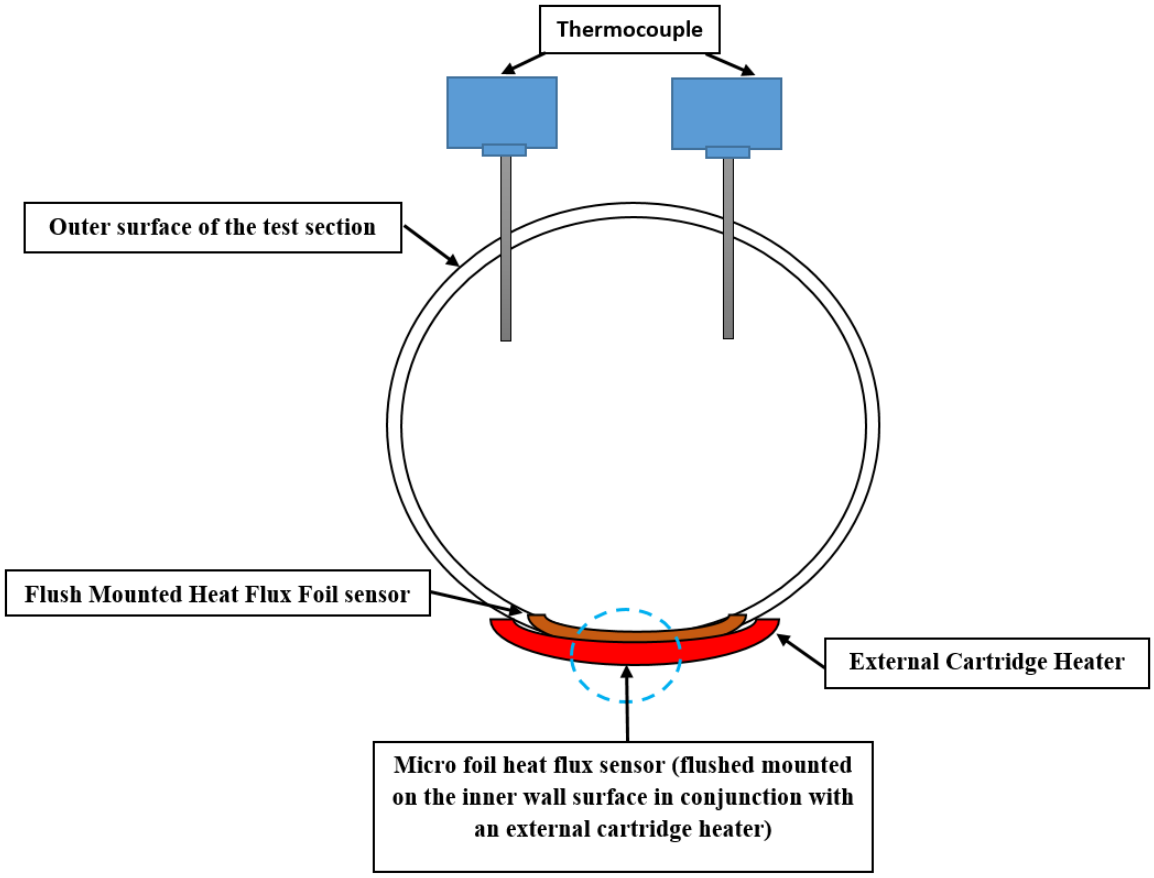


Figure S4: Schematic diagram of the non-invasive heat transfer coefficient probe (flush mounted on the inner wall surface in conjunction with an external cartridge heater)

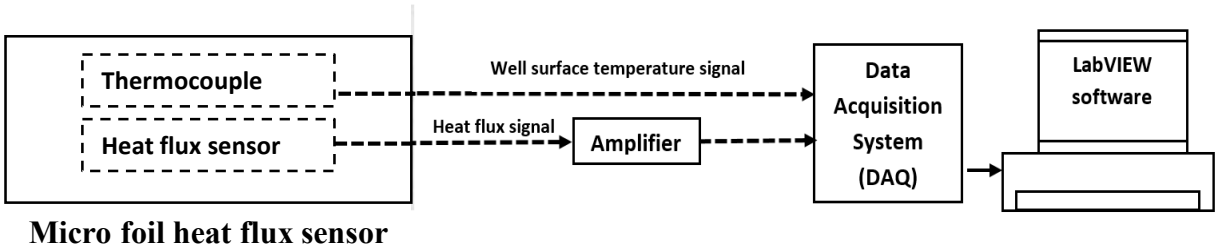


Figure S5: The sequence of the signal collection from the heat flux sensor to the data acquisition system.